Combining gradient ascent search and support vector machines for effective autofocus of a field emission–scanning electron microscope

S. DEMBÉLÉ*,†, O. LEHMANN†, K. MEDJAHER†, N. MARTURI‡ & N. PIAT†
*FEMTO-ST Institute, AS2M Department, Université Bourgogne Franche-Comté, Université de Franche-Comté / CNRS / ENSMM, Besançon, France
†FEMTO-ST Institute, AS2M Department, Université Bourgogne Franche-Comté, Université de Franche-Comté / CNRS / ENSMM, Besançon, France
‡KUKA Robotics, Great Western Street, Wednesbury, U.K.

Key words. Autofocus, gradient ascent search, machine learning, normalized variance, scanning electron microscopy, support vector machines regression.

Summary

Autofocus is an important issue in electron microscopy, particularly at high magnification. It consists in searching for sharp image of a specimen, that is corresponding to the peak of focus. The paper presents a machine learning solution to this issue. From seven focus measures, support vector machines fitting is used to compute the peak with an initial guess obtained from a gradient ascent search, that is search in the direction of higher gradient of focus. The solution is implemented on a Carl Zeiss Auriga FE-SEM with a three benchmark specimen and magnification ranging from x300 to x160 000. Based on regularized nonlinear least squares optimization, the solution overtakes the literature nonregularized search and Fibonacci search methods: accuracy improvement ranges from 1.25 to 8 times, fidelity improvement ranges from 1.6 to 28 times, and speed improvement ranges from 1.5 to 4 times. Moreover, the solution is practical by requiring only an off-line easy automatic train with cross-validation of the support vector machines.

Introduction

The scanning electron microscope (SEM) and the transmission electron microscope (TEM) are reference instruments for the microanalysis of materials: they are widely used in material and life sciences. The autofocus brings to them a significant ease of use especially at high magnifications, its study started two decades ago and led to significant results. It is seen as a problem of optimization. Assuming an unimodal model of the focus with respect to the focal length, it comes to search for the position (focal length) of the maximum of focus (peak). Two types of autofocus can be distinguished.

Correspondence to: Sounkalo Dembélé, FEMTO-ST Institute, AS2M Department, Université Bourgogne Franche-Comté, Université de Franche-Comté / CNRS / ENSMM, 25 rue Savary, 25000 Besançon, France. Tel: +33-381-40-27-91; fax: +33-381-40-28-02; e-mail: Sounkalo.dembele@femto-st.fr

In the first type, people assume an explicit model and use a fitting method to estimate the peak. Nicolls *et al.* (1997) published one of the first work of this type. Assuming a Gaussian model, they computed the peak from two linear equations derived from the ratio of three focus measurements (first, intermediate, last). They also showed that the result was better when the intermediate position is close to the peak. Clearly, for practical issue, this method requires an initial estimation of the peak. Moreover, based on approximated relations, it leads to low accurate results. Rudnaya *et al.* (2012) assumed a quadratic model and used linear least squares fitting to compute the peak from at least three measurements around its initial estimation, which was obtained manually. Unfortunately, standard least squares optimization is known to be sensitive to outliers that come with noise. Nishi *et al.* (2013) assumed a quasi-Gaussian model and used nonregularized nonlinear least squares fitting to estimate the peak from five measurements. Initial peak and model parameter guesses were estimated manually. The method is similar to our method, unfortunately it is not robust to outliers, particularly because of the little number of measurements (sparse data). It fails to give accurate value as soon as one measurement is far from the model. However, we decided to use this method as a benchmark for comparison with our solution.

In the second type of autofocus, people search for the peak of focus without considering any explicit model. To have a reasonable speed, they adopt the coarse-to-fine approach. The peak is searched with lower to higher accuracy. Ong *et al.* (1998a,b) modified hill climbing search by progressively decreasing the sweeping step from far to close to the peak. Batten (2000) implemented a coarse-to-fine approach based on Fibonacci search. Coarse and fine searches were performed at x200 and final magnification (x410, x970, x1350, x26 000), respectively. Marturi *et al.* (2013) published a gradient ascent search method that progressively drives the SEM directly to the peak. These three methods are fast enough but they lack accuracy which is particularly sensitive at high magnifications as in the case of our experiments, up to x160 000.

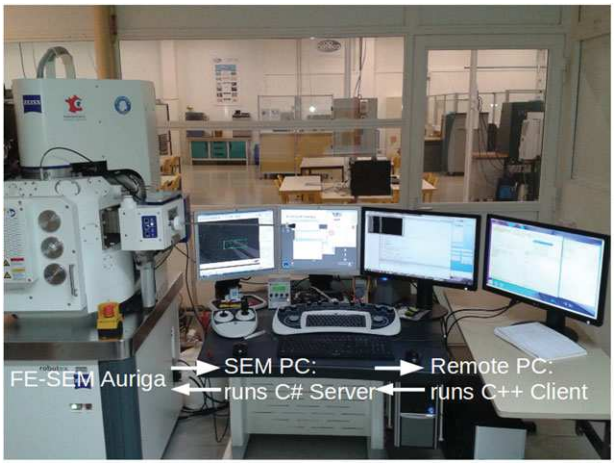

Fig. 1. The setup with the Zeiss Auriga FE-SEM and the associated PC.

This review cannot be ended without considering autofocus in the cases of photon microscope and digital camera. He *et al.* (2003) modified the standard hill climbing search to a coarse-to-fine search. Adaptive big sweeping steps were used to find coarsely the peak where as a constant small step was used to determine it finely. This is somewhat similar to the approach of Ong *et al.* (1998a,b) except that they used square of gradient as focus measure instead of autocorrelation. Wu *et al.* (2012) used the standard hill climbing search to get the initial estimation of the peak. They assumed an exponential model of the focus left and right of that point (quasi-Laplace model), and used linear least squares regression to find the both models. The peak was then computed accurately by the intersection of the both exponentials. The weakness of the method is the lack of robustness to outliers, however it is used as benchmark for comparison with our method. Mir *et al.* (2015), unlike above publications, considered the case of multimodal model and implemented a machine learning-based coarse-to-fine search to find all the peaks, typically the foreground and background. This method does not fall with the scope of this study, which is the unimodality of the model; indeed, our specimens are such they can be imaged at one time by the SEM.

This paper investigates autofocus of the SEM, precisely a Zeiss Auriga FE-SEM. The developed solution combines the advantage of coarse-to-fine search, that is speed, with those of machine learning fitting search (support vector machines or SVM), that is accuracy and fidelity. Gradient ascent search, a native coarse-to-fine search, known for its speed, is chosen to find the initial guess of the focus maximum position. It overtakes the methods presented above (Ong *et al.* 1998a,b;

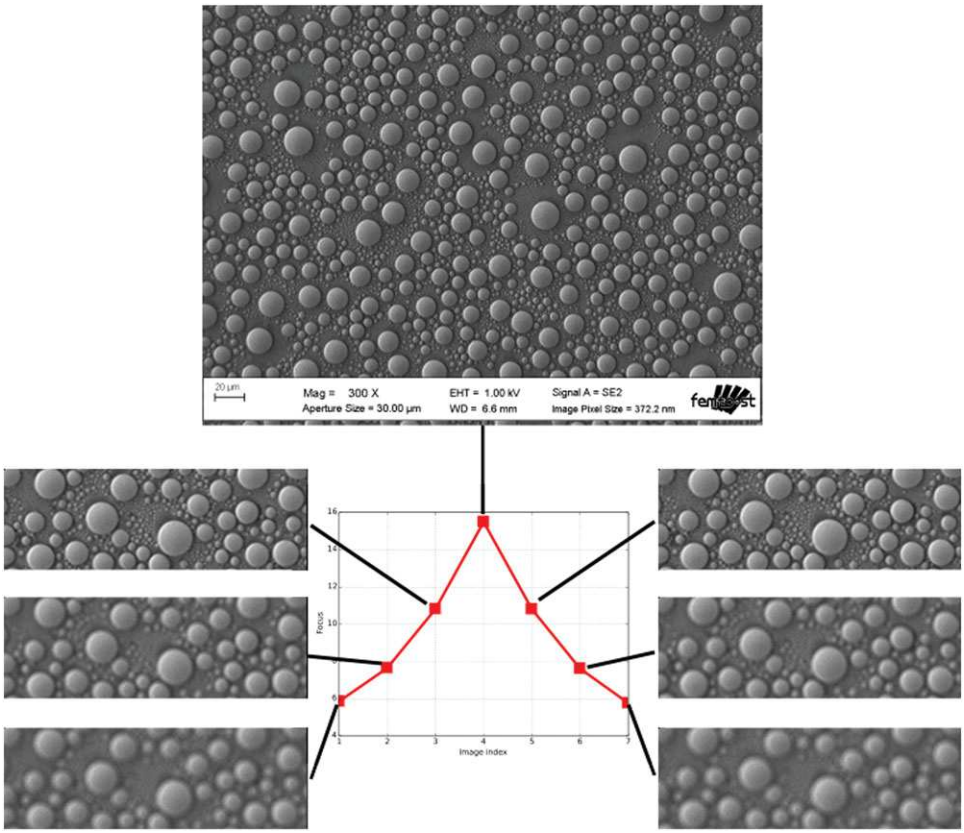

Fig. 2. Illustration of the normalized variance as focus with the tin-on-carbon specimen at x300: the image with the maximum of focus is shown completely, the others are shown partially (cropping of an region-of-interest).

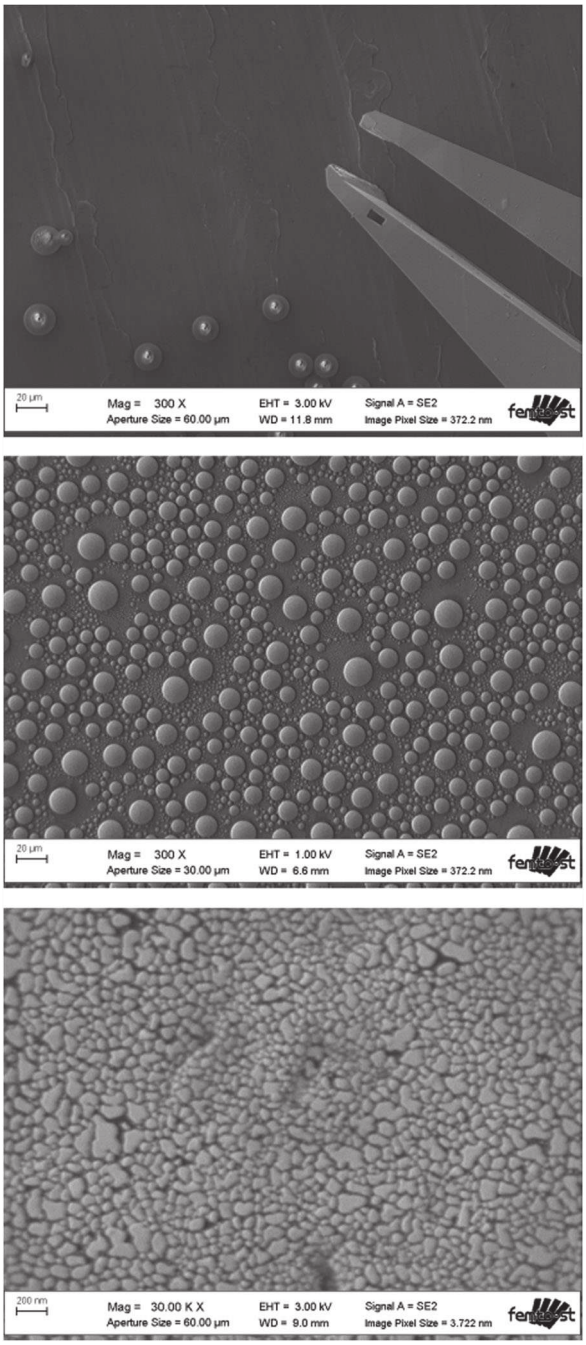

Fig. 3. Experimental benchmark specimens: gold-coated gripper over 20 μm balls (top), tin-on-carbon 5-30 μm particles (middle), gold-on-carbon 5-150 nm particles (bottom).

Batten, 2000; Wu *et al.*, 2012) in term of speed, and of starting point that can be far from the peak. SVMs are chosen for fitting search. Its advantages include accuracy like least squares (Nicolls *et al.*, 1997; Rudnaya *et al.*, 2012; Wu *et al.*, 2012; Nishi *et al.*, 2013), but it overtakes the latter in term of robustness to outliers coming from noise. Indeed, it uses a regularization parameter C that limits the values of the model parameters and more particularly the slack parameter ϵ that tunes the acceptable variations of the data (Bishop, 2006). It is easier to implement than the method of Mir *et al.* (2015), since it is just a regression and only requires an off-line automatic training to determine its parameters. Finally, the solution is an efficient autofocus method that works well at low and high magnifications.

Problem statement

The setup consists of a Zeiss Auriga FE-SEM (Oberkochen, Germany) along with its computer (SEM computer) and a remote computer (Fig. 1). The SEM features Schottky field emission Gemini electron column and two SE detectors (Everhart–Thornley in the chamber and Inlens in the column). The remote computer runs C++ client applications whereas the SEM computer runs C# server applications. The autofocus is implemented as a client application and is based on OpenCV (Bradski, 2000), and particularly the Machine Learning Library which includes the SVM implementation of Chang and Lin (2001).

The focusing in this SEM consists of the direct control of the focal length F. The literature (Batten, 2000; Rudnaya *et al.*, 2010; Marturi *et al.*, 2013) demonstrates the superiority of variance over others focus measures (gradient, autocorrelation, and so on) in terms of speed, accuracy and fidelity. Then we chose normalized variance as focus measure (Fig. 2). Let $I(u, v)$ be the image intensity at the pixel (u, v), the focus measure S may be written:

$$S = \frac{1}{WH\mu} \sum_{W} \sum_{H} (I(u, v) - \mu)^2, \tag{1}$$

with W, H and μ the width, height and mean intensity of the image I, respectively.

Assuming the specimen is installed inside the SEM at an unknown position with the settings (brightness, contrast, astigmatism, scan speed) defined, the problem is how to drive the instrument to the peak of focus. The expected properties are accuracy, robustness to outliers coming with noise and flexibility.

Three benchmark specimens were used to validate the solution: a gold-coated gripper over 20 μm polymer balls on aluminium substrate, tin-on-carbon (5–30 μm particles) and gold-on-carbon (5–150 nm particles) test specimens (Fig. 3).

Developed solution

The block diagram of the solution is depicted in Figure 4. The main stages include coarse-to-fine search for the initial guess of peak position, by means of the gradient ascent search and ultra-fine search, for the final peak position, by means of SVM fitting. Both the stages are performed at predefined lower

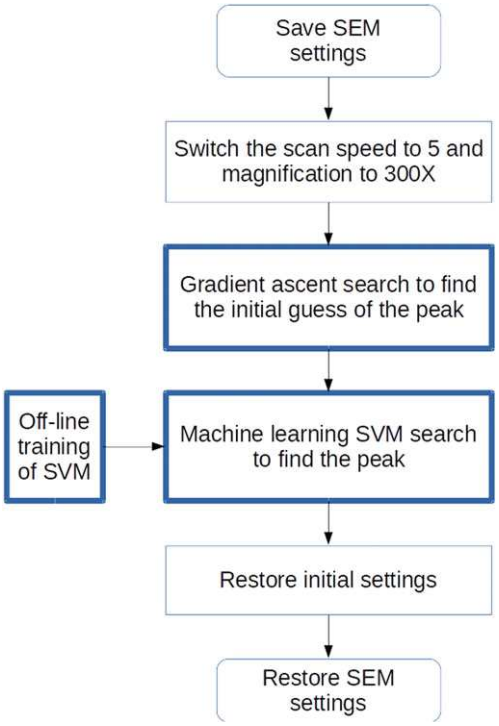

Fig. 4. Block diagram of the developed solution.

region of interest, magnification and scan speed, and at the end, the original settings are restored.

The gradient ascent search method formerly described and applied to a thermo-SEM working at low magnifications by Marturi *et al.* (2013) is revisited. It consists in moving the SEM to the peak of focus by steps relative to the focus: the step is great far from the peak and decreases progressively when approaching the peak.

Let S_k and Δ_k be the focus and the step at the iteration k. Δ_k is written as:

$$\Delta_k = \Gamma_k \, \Lambda_k, \tag{2}$$

with Γ_k the direction of motion,

$$\Gamma_k = \frac{\nabla S_k}{||\nabla S_k||},$$

and Λ_k the decreasing factor,

$$\Lambda_k = \begin{cases} \alpha \left(\frac{S_0}{S_k}\right)^2 & \text{if} \quad \left(\frac{S_0}{S_k}\right) < 1. \\ \alpha & \text{else} \end{cases}$$

The parameter α enables to tune the speed of focusing: the highest is this parameter, the fastest is the autofocus but the highest will be the level of instability. The value of α is empirically chosen as the 3/2 of the depth of field.

From the current focal length F_k, the next focal length F_{k+1} is defined by

$$F_{k+1} = F_k + \Delta_k. \tag{3}$$

The control is stopped when the peak of variance is reached, which is detected by the zero-crossing of its derivative with respect to focal length (Fig. 5). That value defines the initial guess of the peak position, that is it is used for the SVM fitting.

SVM is a convex optimization method to estimate a linear model (Smola & Scholkopf, 2004; Bishop, 2006):

$$y(x) = \boldsymbol{\omega}^{\mathrm{T}} \, \Phi(x) + b, \tag{4}$$

with y is the output or labelled data, x is the input or training data, ω is the vector of model parameters, b is the bias parameter and Φ is the vector of kernel functions.

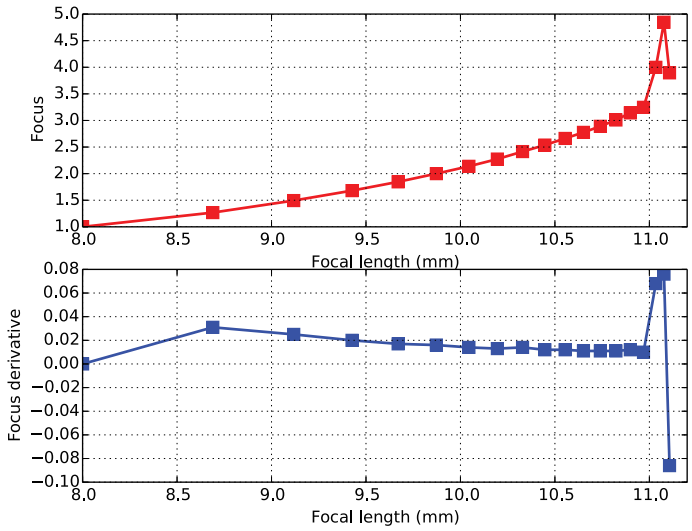

Fig. 5. Gradient ascent search illustration with the gold-on-carbon specimen at x300.

A regularized error function is minimized:

$$C \sum_{k=1}^{N} E_{\epsilon}\left(y\left(x_k\right)-t_k\right)+\frac{1}{2}||\omega||^2 \tag{5}$$

with C is the regularization parameter, t_k is the target value of $y(x_k)$, ϵ is the slack parameter, N is the number of samples and E_ϵ is the ϵ-insensitive error function:

$$E_{\epsilon}\left(y\left(x_k\right)-t_k\right)=\begin{cases}0 & \text{if } \left|y\left(x_k\right)-t_k\right|<\epsilon \\ \left|y\left(x_k\right)-t_k\right| & \text{otherwise}\end{cases}. \tag{6}$$

The problem is solved from Lagrangian multipliers a_k and $\hat{a}_k$:

$$\boldsymbol{\omega}=(\ldots;a_k-\hat{a}_k;\ldots)\;;\; b=\frac{1}{N}\sum_{k} t_k-\epsilon-\boldsymbol{\omega}^{\mathrm{T}}\Phi\left(\mathrm{x}_k\right). \tag{7}$$

The regularization parameter C avoids overfitting, that is avoid the values of the model parameters to reach large values. The slack parameter ϵ determines the admitted variations in the values of the input data with respect to the model. The both parameters, C and ϵ, explain the robustness of SVM (Bishop, 2006) over nonregularized least squares.

SVM is known to fit sparse training data, that is the estimation of new inputs only depends on the kernel to be evaluated at few training points. We use the ϵ-support vector regression with a radial basis function kernel:

$$\Phi_i\left(x_k,\, z_k\right)=e^{-\gamma\|x_k-z_k\|^2}. \tag{8}$$

The three parameters, C, ϵ and γ, have to be estimated accurately, for that a gradient ascent search is first performed to get peak position, several images (301) are acquired around that position from which training (position) and labels (focus) data are generated. Following the references Chang and Lin (2001) and Smola and Scholkopf (2004), an automatic train including a cross-validation is performed to get the parameter values.

With the values of C, γ and ϵ, the SVM is trained from the data of seven images to compute the model from which the peak position (best focal length) is derived.

In addition to our solution, four benchmark solutions were considered. The first was an expert of the microscope who daily used it. The second method was the Zeiss solution that comes with their application development kit. It main stages comprises coarse autofocus by searching from 0 to 20 mm (full focal length range) to find the initial guess of peak, and fine autofocus around that position by Fibonacci searches over increasing magnifications. The third solution was that of Nishi *et al.* (2013). They manually estimated the initial guess of the peak, and assuming a quasi-Gaussian model ($a\ \exp(-\frac{|x-b|^{1.3}}{d})+c$), they used nonregularized nonlinear least squares search to find the peak. The last benchmark was the solution of Wu *et al.* (2012). They used hill climbing search for initial guess. Assuming an exponential model at the left of the peak ($a_l\ e^{b_l x}$), and at the right of the peak ($a_r\ e^{b_r x}$), they used nonregularized nonlinear least squares search to find both models and to compute the peak by their intersection.

Table 1. Comparison of method accuracy with the gripper over 20-μm polymere balls on aluminium substrate ($\times$ means the data were not available).

Magnification	Scan speed (ns/pixel)	Focus				
		FEMTO	WU	NISHI	ZEISS	EXPERT
300	155.5	2.697	2.394	2.559	**3.040**	2.519
	480.5	2.912	2.326	2.710	**3.271**	2.636
	1780	3.169	2.292	2.911	**3.536**	2.878
900	155.5	**4.928**	2.935	3.519	4.615	3.768
	480.5	**6.203**	2.974	4.344	5.537	4.901
	1780	**6.430**	2.977	4.258	5.652	4.936
1200	155.5	**7.175**	3.767	5.002	6.507	5.468
	480.5	**9.130**	4.025	6.397	7.801	7.299
	1780	**9.447**	4.081	6.077	7.976	7.213
1500	155.5	8.868	4.450	6.369	**9.074**	6.927
	480.5	**10.877**	4.800	7.569	10.305	8.644
	1780	**10.756**	4.898	7.008	10.264	8.252
2100	155.5	**11.632**	x	x	11.521	9.152
	480.5	**13.909**	x	x	13.553	11.453
	1780	**15.565**	x	x	15.285	12.706
	Average	**8.247**	3.493	4.894	7.862	6.583

Table 2. Comparison of method fidelity with the gripper over 20-μm polymere balls on aluminium substrate ($\times$ means the data were not available).

Starting point (mm)	Peak position/focal length (mm)				
	FEMTO	WU	NISHI	ZEISS	EXPERT
10	11.059	11.034	**11.080**	x	x
9	11.017	11.105	**11.037**	x	x
8	11.079	11.089	**Failed**	x	x
7	11.068	11.127	**11.078**	11.057	x
6	11.075	11.115	**11.078**	x	11.058
Average	11.059	11.094	**11.068**	x	x
SD	0.025	0.036	**0.021**	x	x

We replaced manual and hill climbing of the last two methods, respectively, by our gradient ascent search and only implemented the fitting stages.

The results of the four methods are compared with our solution, called FEMTO in the tables.

Results

The first experiment was performed with the gold-coated gripper over 20-μm polymere balls on an aluminium substrate, the final objective was the handling of the balls. The following stable settings were used: secondary electron detector, 3 kV voltage, 60 μm aperture, 49.8% brightness (i.e. the ratio of image intensity mean with respect to 255) and 19.6% contrast

Table 3. Comparison of method accuracy with the tin-on-carbon specimen

Magnification	Scan speed (ns/pixel)	Focus			
		FEMTO	WU	NISHI	ZEISS
	155.5	12.231	8.376	3.585	**12.332**
3000	480.5	12.845	7.82	2.806	**13.102**
	1780	12.864	7.442	2.398	**13.195**
	155.5	16.548	10.47	2.552	**17.128**
9000	480.5	16.598	9.698	1.735	**17.492**
	1780	16.392	9.307	1.324	**17.388**
	155.5	9.582	1.968	1.418	**9.934**
30 000	480.5	9.124	1.158	0.638	**9.505**
	1780	8.734	0.753	0.245	**9.127**
	155.5	11.319	1.69	1.406	**11.546**
60 000	480.5	10.781	0.89	0.627	**11.063**
	1780	10.405	0.481	0.234	**10.723**
	155.5	9.143	1.584	1.406	**9.218**
90 000	480.5	8.474	0.787	0.624	**8.6**
	1780	8.097	0.379	0.229	**8.216**
	155.5	6.589	1.516	1.399	**7.741**
120 000	480.5	5.814	0.717	0.621	**7.155**
	1780	5.402	0.311	0.227	**6.786**
	155.5	4.455	1.471	1.395	**6.69**
160 000	480.5	3.524	0.675	0.619	**6.039**
	1780	3.095	0.27	0.226	**5.659**
	Average	9.620	3.227	1.224	**10.411**

(i.e. the ratio of the higher image intensity with respect to the lower intensity).

To evaluate the accuracy of the method, the autofocus was performed at x300 and the magnification was switched to x900, x1200, x1500 and x2100, respectively, and at each magnification the scan speed took the value 155.5 ns/pixel (noisy images), 480.5 ns/pixel and 1780 ns/pixel (sharp images), respectively. In every case, the focus was computed. The results are summarized in Table 1. Except low magnification (x300), our method gives high focus images than any other method. Assuming the accuracy is defined by the value of the focus, these results show that our method overtakes all the other methods. It is slightly better than Zeiss method, 2 times, 1.5 time, and 1.25 time better than Wu method, Nishi method and Expert, respectively.

To evaluate the fidelity of the focal length obtained, we changed the starting point of the autofocus to 10, 9, 8, 7 and 6 mm, respectively. The results are summarized in Table 2, where it can be seen that our method has a standard deviation in the measurement of the focal length of 0.025 mm versus 0.021 mm for Nishi method. Unfortunately, the latter fails in some cases, for example 8 mm. The method is 1.44 time better than the Wu's method.

For a starting point of 8 mm, the speed of the autofocus were 11 s, 33 s, 40 s (+ eventually 10 s for extra fine autofocus) for our method, Expert and Zeiss, respectively: our method is the fastest.

Table 4. Comparison of method fidelity with the tin-on-carbon specimen balls (x means the data were not available)

Starting point (mm)	Peak position/focal length (mm)				
	FEMTO	WU	NISHI	ZEISS	EXPERT
8	**9.278**	9.274	9.278	**9.261**	
7	**9.288**	9.291	Failed	**9.244**	9.291
6	**9.255**	9.462	8.037	**9.261**	x
4	**9.273**	9.332	Failed	**9.278**	x
Average	**9.274**	9.340	8.657	**9.261**	x
SD	**0.014**	0.085	0.877	**0.014**	x

Table 5. Comparison of method accuracy with the gold-on-carbon specimen

Magnification	Scan speed (ns/pixel)	Focus			
		FEMTO	WU	NISHI	ZEISS
	155.5	**3.899**	1.863	1.806	3.348
3000	480.5	**5.402**	0.925	0.868	4.164
	1780	**6.437**	0.440	0.378	4.683
	155.5	**7.032**	1.852	1.828	5.203
9000	480.5	**10.030**	0.920	0.884	6.643
	1780	**12.155**	0.429	0.389	7.619
	155.5	**6.681**	1.928	1.887	4.788
30 000	480.5	**7.622**	0.991	0.959	4.776
	1780	**7.676**	0.500	0.470	4.519
	155.5	**6.474**	1.811	1.782	4.075
60 000	480.5	**6.476**	0.882	0.858	3.502
	1780	**6.095**	0.398	0.378	3.061
	155.5	**6.168**	1.814	1.721	3.662
90 000	480.5	**5.755**	0.889	0.803	2.935
	1780	**5.305**	0.409	0.327	2.490
	155.5	**6.227**	1.840	1.691	3.746
120 000	480.5	**5.604**	0.918	0.781	2.962
	1780	**5.166**	0.435	0.305	2.535
	155.5	**6.141**	1.866	1.692	3.949
160 000	480.5	**5.451**	0.946	0.781	3.160
	1780	**4.984**	0.465	0.305	2.722
	Average	**6.513**	1.072	0.995	4.026

The second experiment was performed with the tin-on-carbon test specimen. The stable settings were: secondary electron detector, 3 kV voltage, 60 μm aperture, 50.4% brightness and 22.3% contrast.

For accuracy evaluation, the autofocus was performed at x300 and the magnification was switched to x3000, x9000, x30 000, x60 000, x90 000, x120 000 and x160 000, respectively, and the scan speed was switched to 155.5 ns/pixel (noisy images), 480.5 ns/pixel and 1780 ns/pixel (sharp

Table 6. Comparison of method fidelity with the gold-on-carbon specimen balls (x means the data were not available)

Starting point (mm)	Peak position/focal length (mm)				
	FEMTO	WU	NISHI	ZEISS	EXPERT
7	**8.946**	8.993	9.035	8.945	8.953
6	**8.943**	8.858	8.948	x	x
5	**8.951**	9.057	8.947	8.955	x
4	**8.947**	9.053	8.924	8.954	x
Average	**8.947**	8.990	8.964	8.951	x
SD	**0.0033**	0.0929	0.0489	0.0055	x

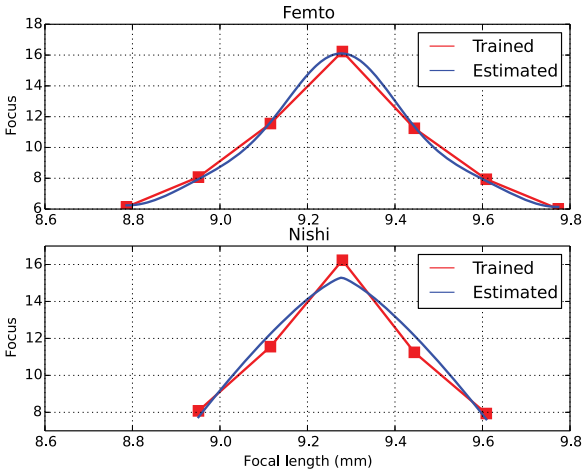

Fig. 6. Our method vs. Nishi's method when the trained points were closed to the model, both methods located the peak at 9.278 mm.

images), respectively. The results are summarized in Table 3. Our method is slightly less better than Zeiss method, but three and eight times better than Wu's and Nishi's methods, respectively.

For fidelity evaluation, the starting point was changed to 8, 7, 6 and 4 mm, respectively. The results are summarized in Table 4. Our method has the same standard deviation of Zeiss method, that is 0.014, that is six times better than Wu's and Nishi's methods.

For a starting point of 10 mm, the speed of the autofocus were 13, 30 and 40 s (+ eventually 10 s for extra fine autofocus) for our method, Expert and Zeiss, respectively: our method overtakes all the other methods.

The third experiment was performed with the gold-on-carbon test specimen. The same procedure was used as the previous experiment.

Table 5 summarized the accuracy of the methods. Our method overtakes all the other method: it is 6, 6.5 and 1.6 time better than Wu's, Nishi's and Zeiss's methods, respectively.

Table 6 summarized the fidelity of the methods. Our method overtakes all the other methods: it is 28, 14, and 1.6 time better than Wu's, Nishi's and Zeiss's methods, respectively.

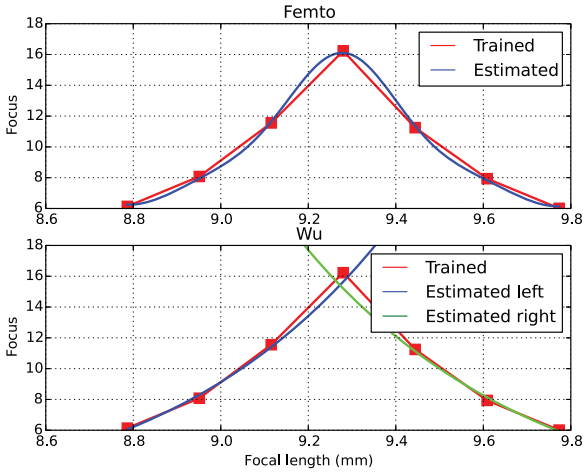

Fig. 7. Our method vs. Wu's method when the trained points were closed to the model, our method and Wu's method located the peak at 9.278 and 9.274 mm, respectively, that is an error of 0.4%.

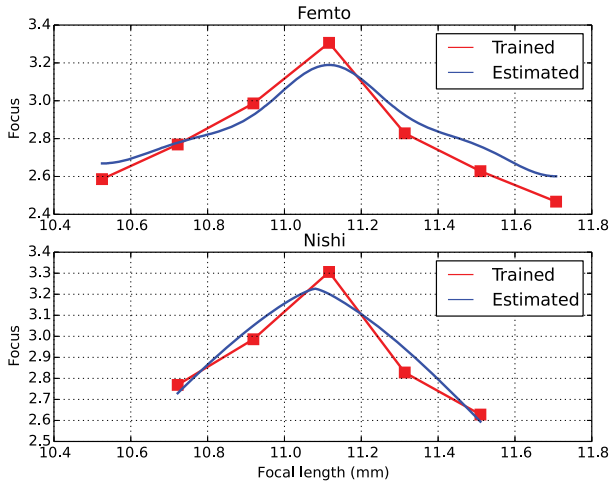

Fig. 8. Our method vs. Nishi's method when one trained point was far from the model, that is an outlier, our method and Nishi's method located the peak at 11.059 and 11.080 mm, respectively, that is an error of 2% of Nishi's method to locate the peak.

For a starting point of 7 mm, our method overtakes the other methods with a speed of 10, 15 and 40 s (+ eventually 10 s for extra fine autofocus) for our method, Expert and Zeiss, respectively.

Above results can be easily explained. If the model is close to the trained points, the three methods (our, Wu's and Nishi' methods) find the peak with high accuracy (Figs. 6 and 7). This is normal because the three methods are based on nonlinear least squares optimization. In the other cases, that is presence of outliers Nishi's method gives inaccurate peak (Fig. 8) or fails to find the peak (Fig. 9). Wu's method also gives inaccurate peak (Fig. 10), but does not failed.

Finally, our method out-performs all the other methods with respect to accuracy and fidelity of measurements.

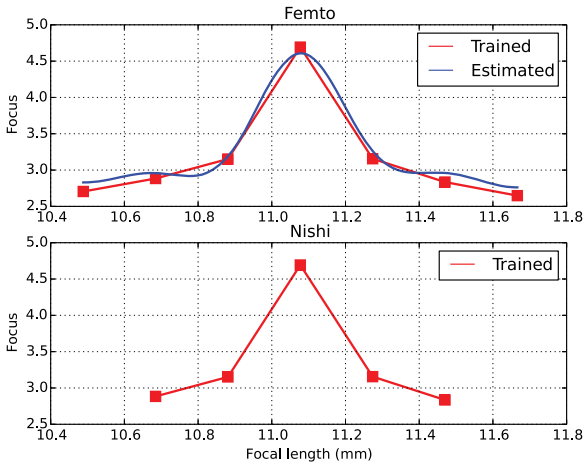

Fig. 9. Our method vs. Nishi's method when two trained points were far from the model, our method located the peak at 11.079 mm and Nishi's method failed.

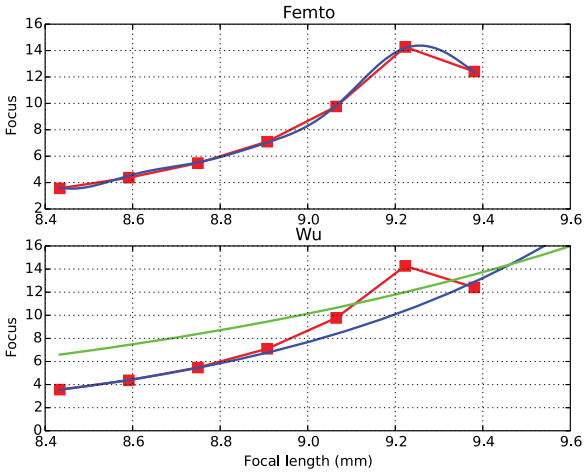

Fig. 10. Our method vs. Wu's method when the trained points were not symmetric with respect to the peak guess, our method and Wu's method located the peak at 9.255 and 9.462 mm, respectively, that is an error of 2%.

Conclusion

The paper has investigated the problem of autofocus in SEM. A solution is developed that combines gradient ascent search, a native coarse-to-fine search approach, to find the peak of focus, with the machine learning SVM fitting, a regularized and nonlinear least squares optimization method, of seven focus data to compute the peak. It has been applied to a Carl Zeiss Auriga FE-SEM with three specimen, a gold-coated gripper over 20 μm polymere balls on an aluminium substrate, a tin-on-carbon test specimen with 5–30 μm particles and a gold-on-carbon test specimen with 5–150 nm particles.

The results have shown an improvement of accuracy with respect to literature nonregularized optimization methods and Fibonacci search method ranging from 1.25 to 8 times. The improvement of fidelity ranged from 1.6 to 28 times, that of speed from 1.5 to 4 times.

Finally, the work led to a practical and efficient autofocus method for electron microscopes and probably for other imaging systems. The main drawback of this solution is the gradient ascent search, which gives the initial guess of peak, it sometimes gets stuck at local maxima. An improvement would come with the use of a robust method like Newton's method.

Autofocus is interesting for standard SEM use: analysis of specimen from 2D images. It becomes essential for the real-time depth estimation during robotic handling of specimen, Fatikow *et al.* (2007), and more particularly for the reconstruction of 3D images by means of the structure-from-motion approach: rotation of the specimen under the electron column, acquisition of focused images, processing of images and reconstruction of the 3D mode, Kratochvil *et al.* (2010). At high magnification, the focus can get lost during image acquisition and it is required to perform an autofocus.

Acknowledgements

The authors thanks Julien Derivet for his participation and the team ROBOTEX for their support.

Funding Source

This work has been supported by the Equipex ROBOTEX project (contract No. ANR-10-EQPX-44-01), the Labex ACTION project (contract No. ANR-11-LABX-0001-01) and the NANOROBUST project (contract No. ANR-11-NANO-006).

References

Batten, C.F. (2000) Autofocusing and astigmatism correction in the scanning electron microscope. Master's thesis, University of Cambridge, Cambridge, UK.

Bishop, C.M. (2006) *Pattern Recognition and Machine Learning*. Springer, New York, USA.

Bradski, G. (2000) The OpenCV Library. *Doctor Dobbs Journal* **25**(11), 120–126.

Chang, C.-C. & Lin, C.-J. (2001) Libsvm: a library for support vector machines. *ACM Trans. Intell. Sys.Technol.* **2**(27), 1–27.

Fatikow, S., Wich, T., Hülsen, H., Sievers, T. & Jähnisch, M. (2007) Microrobot system for automatic nanohandling inside a scanning electron microscope. *IEEE/ASME Trans.* **12**, 244–252.

He, J., Zhou, R. & Hong, Z. (2003) Modified fast climbing search autofocus algorithm with adaptive step size searching technique for digital camera. *IEEE Transactions on Consumer Electronics* **12**, 244–252.

Kratochvil, B.E., Dong, L.X., Zhang, L. & Nelson, B.J. (2010) Image-based 3D reconstruction using helical nanobelts for localized rotations. *J. Microsc.* **237**, 122–135.

Marturi, N., Tamadazte, B., Dembélé, S. & Piat, N. (2013) Visual servoing-based approach for efficient autofocusing in scanning electron microscope. In *Proceedings of the 2013 IEEE/RSJ International*

Conference on Intelligent Robots and Systems (IROS), Tokyo, pp. 2677–2682.

Mir, H., Xu, P., Chen, R., & van Beek, P. (2015) An autofocus heuristic for digital cameras based on supervised machine learning. *Journal of Heuristics* **21**(5), 599–622.

Nicolls, F.C., de Jager, G. & Sewell, B.T. (1997) Use of a general imaging model to achieve predictive autofocus in the scanning electron microscope. *Ultramicroscopy* **69**(1), 25–37.

Nishi, R., Moriyama, Y., Yoshida, K., Kajimura, N., Mogaki, H., Ozawa, M. & Isakozawa, S. (2013) An autofocus method using quasi-Gaussian fitting of image sharpness in ultra-high-voltage electron microscopy. *Microscopy* **62**(5), 515–519.

Ong, K.H., Phang, J.C.H. & Thong, J.T.L. (1998) A robust focusing and astigmatism correction method for the scanning electron microscope. Part II: Autocorrelation-based coarse focusing method. *Scanning* **20**, 324–334.

Ong, K.H., Phang, J.C.H. & Thong, J.T.L. (1998) A robust focusing and astigmatism correction method for the scanning electron microscope - Part III: an improved technique. *Scanning* **20**, 357–368.

Rudnaya, M.E., Mattheij, R.M.M. & Mauback, J.M.L. (2010) Evaluating sharpness functions for automated scanning electron microscopy. *J. Microsc.* **240**(1), 38–49.

Rudnaya, M.E., ter Morsche, H.G., Maubach, J.M.L. & Mattheij, R.M.M. (2012) A derivative-based fast autofocus method in electron microscopy. *J. Mathe. Imag. Vis.* **44**, 38–51.

Smola, A.J. & Scholkopf, B. (2004) A tutorial on support vector regression. *Stat. Comp.* **14**, 199–222.

Wu, Z.M., Wang, D.H. & Zhou, F. (2012) Bilateral prediction and intersection calculation autofocus method for automated microscopy. *J. Microsc.* **2048**(3), 271–280.